ELSEVIER

Graphene nano-heterostructures for quantum devices

D. Bischoff*, M. Eich, A. Varlet, P. Simonet, H.C. Overweg, K. Ensslin and T. Ihn

Solid State Physics Laboratory, ETH Zurich, 8093 Zurich, Switzerland

Ten years ago, the exfoliation of graphene started the field of layered two-dimensional materials. Today, there is a huge variety of two-dimensional materials available for both research and applications. The different dimensionality compared to their bulk relatives is responsible for a wealth of novel properties of these layered two-dimensional materials. The true strength of two-dimensional materials is however the possibility to stack different layers on top of each other to engineer new heterostructures with specifically tailored properties. Known as van-der-Waals heterostructures, they enable the experimental observation of a variety of new phenomena. By patterning the individual layers laterally into nanostructures, additional functionality can be added to the devices. This review provides a glimpse at the future opportunities offered by van-der-Waals stacked nanodevices.

Introduction

The exfoliation of graphene in 2004 with the experimentally cheap and easy ''scotch-tape technique'' [1] opened a whole new research field. Graphene is a monoatomic layer of carbon, making it a truly two-dimensional material [1,2]. It possesses special electronic, mechanical, optical and thermal properties making it a promising candidate for many applications [3–9]. It soon became apparent that many other two-dimensional materials can be fabricated using the same technique [10]. Until today, experiments on a large variety of two-dimensional materials have been reported [11–17]. A basic requirement to fabricate a two-dimensional material is that the bulk crystal consists of layers bound to each other by van-der-Waals forces. The intra-layer atomic structure of these materials can be quite different. Hexagonal boron nitride (hBN), for example, has the same in-plane crystallographic structure as graphene with the carbon atoms replaced alternately by boron and nitrogen atoms [18]. Transition metal dichalcogenides [12], such as tungsten disulfide (WS_2) or molybdenum disulfide (MoS_2), typically consist of three atomic layers bound to each other covalently. There are various other layered materials such as oxides [13] or polymers [16] whose crystal structure is even more complicated.

Over the last years, significant improvements in material preparation were achieved. While in early experiments device sizes and fabrication were limited by the ''scotch-tape technique'', it has recently become possible to grow graphene sheets of nearly unlimited size by chemical vapor deposition (CVD) [19]. The quality of CVD graphene has become comparable to devices obtained from natural graphite [20,21]. The logical next step is the growth of different layered materials on top of each other [22,23], potentially resulting in low-defect density large-area stacks with atomically clean interfaces.

Graphene van-der-Waals heterostructures

While these two-dimensional layered materials have interesting properties of their own, the possibility to combine several of them into new heterostructures offers many opportunities. The whole toolbox necessary for fabricating devices is available: there are insulators, semiconductors with various band gaps, semi-metals, metals and superconductors [12,13]. This review focuses on a number of electronical transport experiments where at least one layer of graphene is involved. We start with the simplest graphene-based heterostructures consisting of a graphene sheet on top of another layered material and move on to more complicated device designs. Finally, three experiments will be discussed where one or even two layers within the stack of two-dimensional materials are additionally patterned into nanostructures. These devices of

*Corresponding author: Bischoff, D. (dominikb@phys.ethz.ch)

 http://dx.doi.org/10.1016/j.mattod.2016.02.021

stacked nanostructures are specific examples of a new class of structures that could open completely novel opportunities for realizing (quantum) electronics based on stacked layered materials.

Graphene on a layered material substrate: improved quality

A first significant breakthrough in electronic graphene devices was achieved when the substrate was removed and the resulting suspended graphene sheets were subsequently cleaned by thermal annealing [24,25]. In unsuspended graphene devices, disorder from the commonly used silicon dioxide substrates leads to charge carrier scattering and thereby degrades its electronic properties. However, suspended devices are fragile, limited in device geometry and withstand only small gate voltages before they collapse. An alternative route to obtain graphene with low disorder is to deposit it on a hexagonal boron nitride substrate [26]. Such a device is schematically depicted in Fig. 1a. Hexagonal boron nitride is a two-dimensional crystal with an atomically flat surface and very few crystal defects. Together with a heat-cleaning step, the electronic properties of graphene increased significantly, leading to the observation of broken symmetry [27] and fractional quantum Hall states [28,29]. Also, long-range spin transport [30] and the quantum spin Hall effect [31] were observed in graphene devices on hexagonal boron nitride. The order of the stack was also inverted: hexagonal boron nitride was used as a top-gate dielectric being electronically more stable than the other oxides grown on graphene [32,33]. Beyond hexagonal boron nitride, other layered materials were also investigated in transport experiments [34]: spin–orbit coupling can be induced in graphene on tungsten disulfide substrates [35] and charge can be transferred from graphene to a molybdenum disulfide substrate [36].

Graphene sandwiches

Graphene is an ideal material for fabricating sensors. It has a huge surface-to-volume ratio such that even single molecules can be detected [37]. However, this high sensitivity is a huge disadvantage when the intrinsic properties of graphene are to be investigated. The apparent solution is to protect both sides of the graphene layer from the environment by sandwiching the graphene between two hexagonal boron nitride crystals [38], as shown in Fig. 1b. This encapsulation resulted in an additional improvement of device characteristics and cleanliness [38], enabling the observation and manipulation of spin relaxation in graphene [39,40]. Surprisingly, it was found that interfaces between the graphene and the two hexagonal boron nitride layers were nearly atomically clean [41] despite graphene being exposed to ambient conditions prior to encapsulation [42]. The microscopic mechanism leading to such clean interfaces is so far not fully understood. The fabrication of encapsulated graphene was further improved by a process allowing to contact graphene sheets after stacking the graphene sandwich, thereby preventing graphene from getting in contact with processing-chemicals [43–45].

The encapsulation of bilayer graphene between hexagonal boron nitride also provides the opportunity to apply high vertical electric fields, so-called displacement fields, between a top- and a back-gate in order to open a band gap [46], which was previously done using other dielectrics [47–49]. The graphene quality is an important parameter for opening the band gap. Crystal defects such as grain boundaries can prevent the electrical observation of the gap [50]. High quality double-gated bilayer graphene devices led to the observation of Fabry-Pérot interference [51], a Lifshitz transition [52] and a tunable fractional quantum Hall effect [53]. Recently, also valley currents [54,55] became experimentally accessible, where the lifted valley degeneracy of graphene can be exploited. Further, it was demonstrated that electrons in double-gated bilayer graphene can exhibit properties similar to photons in wave-guides [56]. Patterned top-gates allowed to electrostatically define nanostructures [46] similar to the technologically more complicated suspended bilayer graphene devices [57]. Such a device is depicted in Fig. 1c.

Tunneling through layered materials

As the thickness of insulating layered two-dimensional materials is well defined and homogeneous over large areas and as they are low defect-density crystals, they are the perfect material for tunneling barriers [58–60]. Tunneling barriers made from monolayer hexagonal boron nitride were used to inject spins into graphene devices [61]. Hexagonal boron nitride [62] as well as tungsten disulfide [63] tunneling barriers were used to build tunneling transistors: in those devices, the charge carrier densities in the two graphene sheets being separated by the insulator are modulated, resulting in significantly smaller off-state currents than in conventional graphene field effect transistors [62–64]. Such a tunneling transistor is schematically depicted in Fig. 1d.

Graphene double layers

Taking the complexity of the devices even one step further, double layer graphene devices were fabricated: they consist of two encapsulated graphene layers being separated by a thin dielectric as shown in Fig. 1e. The thin dielectric – typically a few layers of hexagonal boron nitride – is chosen to be thick enough to prevent tunneling from one graphene layer to the other. The average spacing of electrons contributing to transport within each layer can be significantly larger than the distance between the two graphene layers, resulting in strong inter-layer Coulomb interactions. Among the observed phenomena are different drag mechanisms [65,66] where a bias voltage is applied to one layer while the other layer is kept unbiased: momentum transfer of the electrons from the biased layer to electrons in the unbiased layer results in a current flowing at zero bias voltage. Graphene double layers further allowed to investigate Anderson insulation in ultraclean devices where the electrons in each layer partially screen the disorder of the other layer [67].

Relative layer orientation

It was soon realized [68] that the properties of the heterostructures do not only depend on the stacking order, the material and the interface quality, but also on the relative orientation of the layers. When two graphene layers are stacked such that their principal lattice orientations are different, a superlattice emerges due to the appearance of a Moiré-pattern. Such a device is schematically depicted in Fig. 1f. In order to fabricate a superlattice that can be investigated in electronic transport experiments, the mismatch angle needs to be carefully controlled. Similar devices were fabricated experimentally, where a graphene flake was aligned on top of

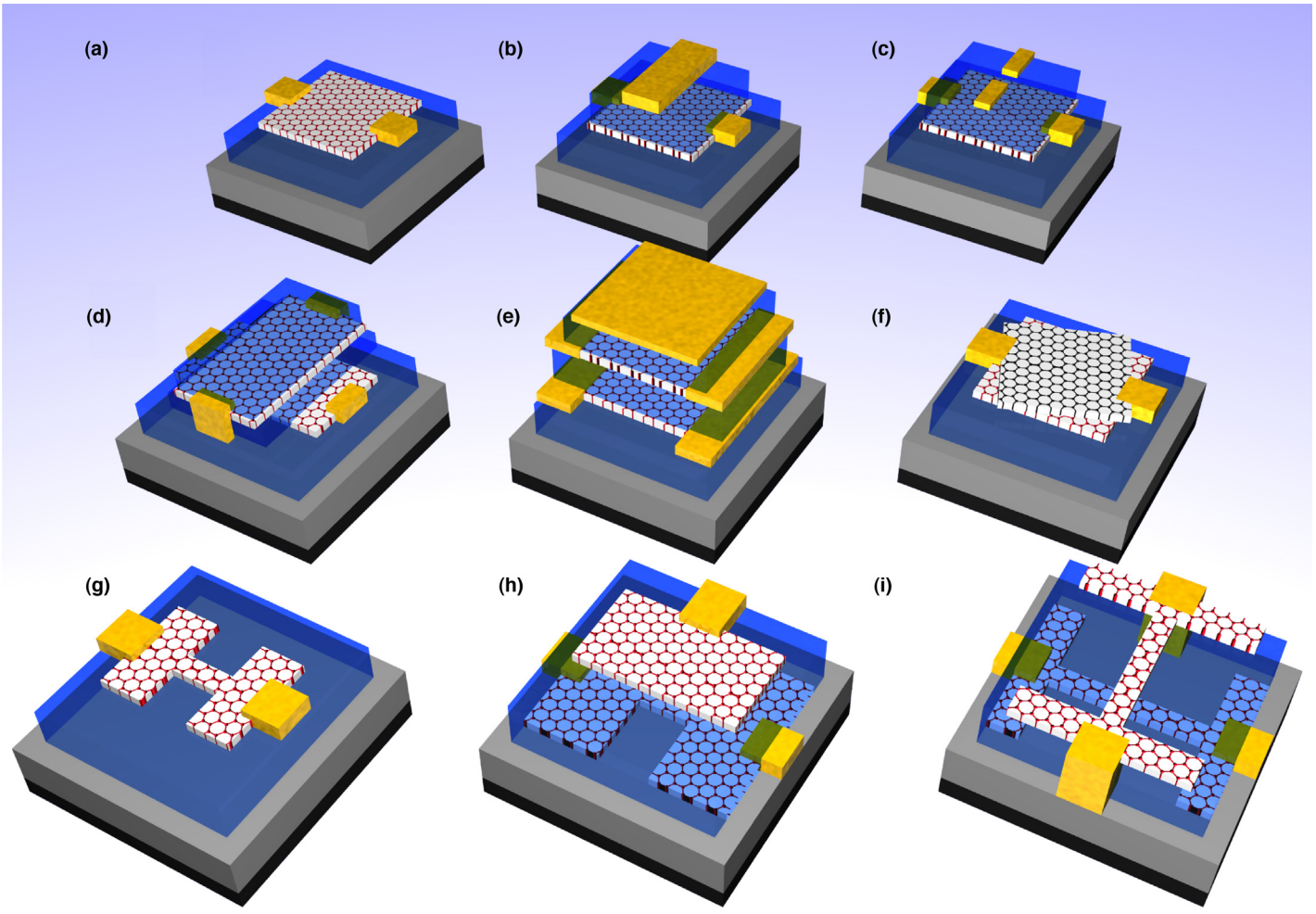

FIGURE 1

Overview of different device geometries consisting of stacked van-der-Waals heterostructures containing at least one layer of graphene: (a) Graphene on a hexagonal boron nitride substrate (blue layer) showing reduced disorder compared to devices directly fabricated on silicon dioxide. (b) Graphene encapsulated in hexagonal boron nitride with a top gate spanning the whole device width. Such geometries can be used to open a band gap in bilayer graphene. (c) Similar as (b) but with two top gates defining an ungated channel. (d) Two graphene layers being separated by a thin hexagonal boron nitride flake: the tunneling current between the two graphene layers can be tuned electrostatically. (e) Similar as in (d) but with a slightly thicker hexagonal boron nitride layer preventing tunneling. Electrons in both layers are coupled to each other by Coulomb interactions. (f) Two graphene layers directly on top of each other, with a slight mismatch of their crystal orientation. Such a structure results in a superlattice due to the Moiré pattern originating from the twist angle. (g) A graphene nanoribbon located on top of a hexagonal boron nitride substrate. The change in substrate allows investigating which sources of disorder are relevant. (h) A graphene sheet separated by hexagonal boron nitride from a graphene nanoribbon. The ribbon can be used as a sensitive detector of the electrochemical potential of the graphene sheet. (i) Two graphene ribbons separated by a thin hexagonal boron nitride layer. Such device geometries allow to investigate charge detection and detector back-action.

an hBN flake. These devices allowed to observe manifestations of the so-called "Hofstadter's Butterfly" [69–71], a long predicted self-similar energy spectrum of a periodic lattice in a magnetic field. In the case of the graphene devices, a number of copies of the principal Dirac cones in the band structure were observed. Related to this change of band structure is also the observation of topological currents in such systems [72,73].

Different two-dimensional conductors

Recently, van-der-Waals stacked devices were also fabricated using different conductive materials. Memory cells as well as transistors were demonstrated using combinations of molybdenum disulfide, hexagonal boron nitride and graphene [74,75]. Atomically sharp PN junctions were realized by combining molybdenum disulfide and tungsten diselenide [76].

The next step: nanostructuring material stacks

The experiments discussed so far showed a wealth of interesting phenomena in devices combining a small number of different layered materials. Using additional layered materials will open many possibilities for future experiments and applications. However, there is another option offering opportunities for new device geometries: the individual layers can be laterally patterned into nanostructures, allowing for further functionality. The remainder of this review will focus on such laterally nano-patterned van-der-Waals heterostructures.

Graphene nanoribbons on hexagonal boron nitride

The conceptually simplest laterally patterned van-der-Waals heterostructures are graphene nanoribbons on a hexagonal boron nitride substrate [78,79], as depicted schematically in Fig. 1g.

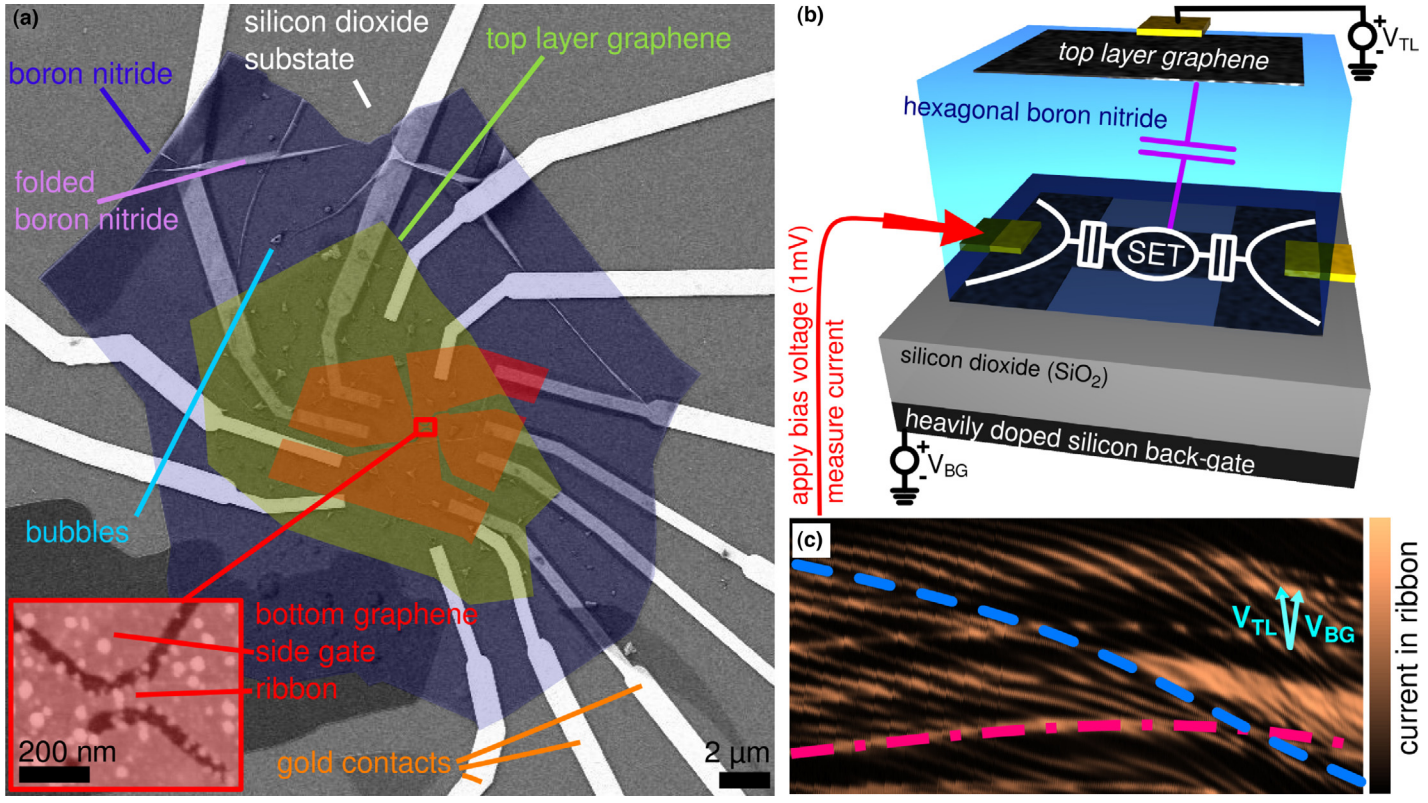

FIGURE 2

(a) False-colored scanning electron microscopy (SEM) image of the device consisting of a graphene nanoribbon (red) separated by a hexagonal boron nitride flake (purple) from the top-layer graphene (green). Fabrication imperfections such as bubbles and wrinkles are visible. The red inset in the lower left corner is a scanning force microscopy (SFM) image of the ribbon, before the hexagonal boron nitride was deposited. (b) Schematic of the device: the graphene nanoribbon acts as a single electron transistor (SET) which is strongly capacitively coupled to the graphene top layer. The graphene SET is therefore a sensitive detector for the density of states of the top layer graphene. By changing the applied voltages V_{TL} and V_{BG}, both the density in the ribbon as well as in the graphene sheet can be changed. (c) Current flowing through the nanoribbon as a function of applied gate voltages (note that the axes are not perpendicular to each other in order to increase the visibility). Curved Coulomb resonances with different slopes are found (two are exemplarily marked by the dashed lines). The bending of the lines is a result of the quantum capacitance of the graphene sheet, changing the overall capacitance between the ribbon and the graphene sheet for low densities in the graphene sheet. The different sets of resonances originate from microscopic fabrication residues at the interfaces between the hexagonal boron nitride and the two graphene layers. Data in (c) are a zoom of the data presented in Ref. [77].

Graphene nanoribbons [80,81] are stripes of graphene with a width of less than 100 nm. Contrary to unpatterned graphene devices, the improved substrate did not result in a significant change of the device characteristics when compared to nanoribbons on SiO_2 substrates [78]. This is because disorder introduced by the rough edges limits charge transport [78] and leads to localization of charge carriers, which is experimentally detected by the observation of Coulomb blockade [82,83]. Similar experiments were also performed with graphene quantum dot devices on hexagonal boron nitride substrates [84].

A graphene nanoribbon coupled to a graphene sheet: probing the quantum capacitance

The localized charge carriers in graphene nanoribbons can be used as sensitive detectors for their electrostatic environment: every charge carrier in the vicinity of the ribbon creates an electric field and will thereby lift the electrostatic potential energy of the localized charge-state in the ribbon. A graphene ribbon separated from a graphene sheet by a thin layer of hexagonal boron nitride can therefore be used to probe the electronic density of states in the graphene sheet using the so-called quantum capacitance [77]. Such a device is schematically shown in Fig. 1h, and a real device is depicted in Fig. 2a,b. The graphene ribbon is in this case used similarly to a single electron transistor (SET) [86–88]. The advantage of using a graphene ribbon is the relatively easy fabrication and the close vicinity of the ribbon to the system under investigation given by the thickness of the hexagonal boron nitride. A thin boron nitride layer results in strong coupling and therefore in an enhanced measurement signal.

When finite density of states corrections are considered beyond bare geometry, the capacitance between two conducting surfaces is given by $C_{total} = (1/C_{geometrical} + 1/C_{quantum})^{-1}$, where the geometrical capacitance only depends on the shape, dimensions, and the separation of the surfaces [89], whereas the quantum capacitance is proportional to the density of states of the conducting surfaces. The quantum capacitance term is negligible in most practical capacitors. In nanoscale capacitors, however, the geometrical capacitance (per area) can become very large and the density of states in the conducting surfaces of the capacitor can become very small, such that the latter dominates the total capacitance. These conditions are for example achieved in graphene – hexagonal boron nitride – graphene heterostructure stacks, where the dielectric boron nitride

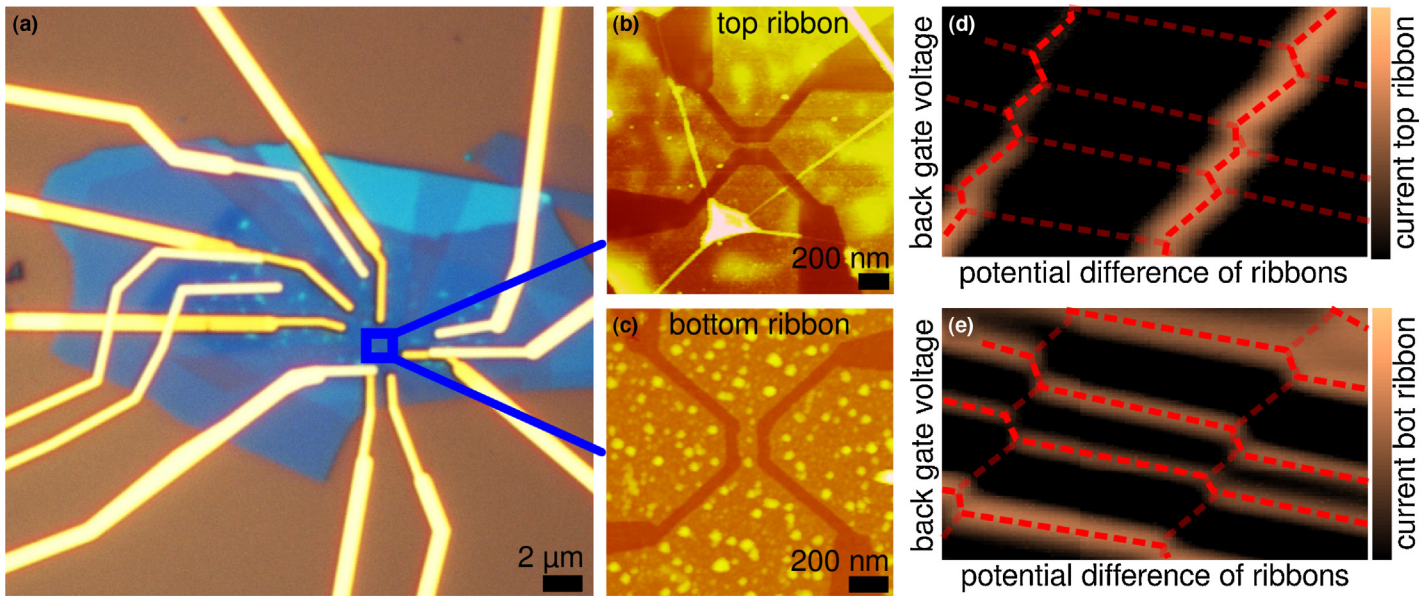

FIGURE 3

(a) Optical microscopy image of a device where two nanoribbons are located on top of each other, separated by a thin dielectric of hexagonal boron nitride. The yellow lines are metal contacts and the blue area is the hexagonal boron nitride flake. The top graphene sheet can be discerned from the hexagonal boron nitride by the bubbles making it appear more rough (middle of blue region). (b,c) Scanning force microscopy images of the top and the bottom graphene nanoribbons. (d,e) Current flowing through the top/bottom graphene ribbon while a small bias voltage is applied separately to each of them. The axes are given by a global back gate voltage and the electrostatic potential difference between the top and the bottom ribbon. The Coulomb blockade resonances – highlighted by red dashed lines – have a kink whenever one resonance in one ribbon crosses a resonance in the other ribbon. Overlaying the red lines from each ribbon results in a hexagonal pattern expected for double quantum dots. The data in (b–e) are the same data as presented in Ref. [85].

layer is chosen to be thin. Such device geometries can for example be used for supercapacitors [90]. A graphene nanoribbon below (or above) the graphene sheet can then be used to obtain local information on the quantum capacitance and therefore on the density of states in the graphene sheet [77]. This allows, for example, to probe disorder in the graphene sheet close to the charge neutrality point by measuring the current flowing through the nanoribbon [77], as shown in Fig. 2c. It was found that microscopic contaminations at the interface between the layers can locally change the thickness of the dielectric and therefore also change the local geometric capacitance [77]. This spatially varying geometric capacitance induces inhomogeneities in the charge carrier distribution that can be larger than the intrinsic disorder [77]. It is therefore crucial for van-der-Waals heterostructures to have atomically clean interfaces to ensure high-quality device performance.

Two strongly coupled graphene nanoribbons: a toolbox for charge detection

This method of capacitive detection can not only be used to probe the density of states in a graphene sheet, but also to detect localized charge carriers in nanostructures. Figs 1i and 3a–c show a device where this scheme was implemented. The device consists of two perpendicularly aligned graphene nanoribbons located on top of each other and separated by a thin insulating layer of hexagonal boron nitride [85]. Due to the symmetry of the device, each nanoribbon can be used as a charge detector for the other nanoribbon. The localized charges in each ribbon then act as single electron transistors (or equivalently: quantum dots). This mutual charge detection is visible as kinks in the Coulomb blockade resonances shown in Fig. 3d–e. If the devices were not coupled

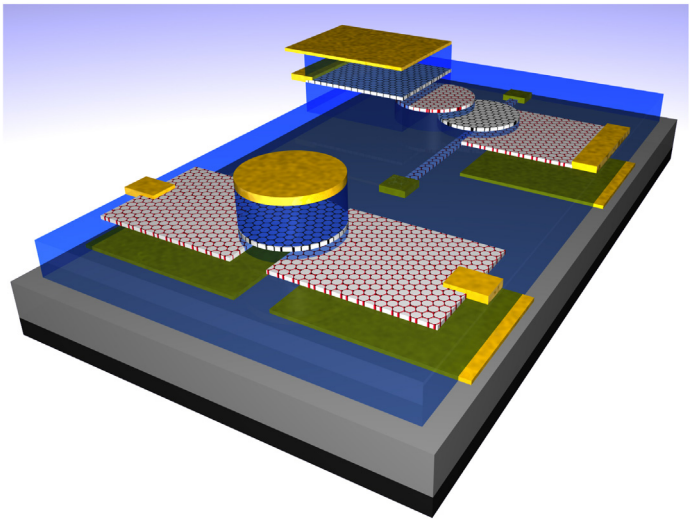

FIGURE 4

Illustration of possible future devices made of nanostructured stacks of layered materials. Front: a conducting island (e.g. graphene) is tunneling coupled to two conducting leads by a thin layer of insulator (e.g. hexagonal boron nitride). A top gate on the island allows tuning its potential. Metal gates below the leads allow to tune the density of the leads and therefore the tunneling coupling strength between the island and the leads. Back: the dot idea is taken one step further. Instead of just having one quantum dot island, a second island is tunneling coupled to it. It would be further possible to couple an additional nanoribbon to one or both of the islands, which could be used as a charge detector to monitor the charge occupancy of the individual dots.

by inter-layer Coulomb-interactions between localized states, each Coulomb resonance would be a straight line in this diagram where two gate voltages are tuned. The slope would reflect the ratio of capacitances between the dot and the two gates. Here these slopes are not straight because adding one electron to one of the dots shifts the energy levels in the neighboring dot hosted in the other graphene ribbon. Such a device can be treated as a capacitively coupled double quantum dot system allowing to investigate the effects of charge detection (by a dot in one of the ribbons) on the measured dot in the other ribbon [85]. These effects are summarized under the term ''measurement back-action''. It was found that sending a current through one ribbon can induce a current in the other ribbon, even if zero bias voltage is applied to the second ribbon [85]. This unexpected result can be explained by energy dependent tunneling rates in graphene single electron transistors and the strong capacitive coupling between the ribbons [91]. By carefully analyzing the induced current, it was further found that additional higher order quantum mechanical processes need to be present to exchange energy between the two ribbons [85,92]. Such a device with two capacitively coupled nanoribbons is therefore an ideal system to study Coulomb-interactions between different graphene nanodevices.

Outlook

The wealth of different layered materials with often unique properties together with the possibility to stack them in any imaginable order leads to a huge number of possible combinations. The difficulty in the future will mostly lie in identifying useful combinations of materials and in fabricating them with the necessary precision. Challenges on the technology side are the quality of the materials themselves, the cleanliness of the interfaces and also the relative alignment of the different materials. As demonstrated in this review, additional opportunities for devices arise when individual layers of such a stack are nano-patterned laterally. One peculiarity of laterally patterned graphene nanodevices fabricated so far is, that reproducible lateral tunneling barriers are hard to achieve [79,93,94]. This issue could be addressed by using a thin layer of an insulator as a vertical tunneling barrier. The tunability of the tunneling coupling could then for example be achieved by tuning the charge carrier density of the leads. Two possible future devices following this idea are depicted and described in detail in Fig. 4. Beyond the electronic devices discussed in some detail in this review, van-der-Waals heterostructures of (nanostructured) layered materials offer many opportunities to engineer devices for optical applications, sensors, energy storage and many other applications [95].

Acknowledgements

Financial support by the National Center of Competence in Research on ''Quantum Science and Technology'' (NCCR QSIT) funded by the Swiss National Science Foundation, by the Marie Curie ITNs S^{3}NANO and QNET is gratefully acknowledged.

References

[1] K.S. Novoselov, et al. Science 306 (2004) 666–669.
[2] A.K. Geim, K.S. Novoselov, Nat. Mater. 6 (2007) 183–191.
[3] K.S. Novoselov, et al. Nature 438 (2005) 197–200.
[4] Y. Zhang, et al. Nature 438 (2005) 201–204.
[5] C. Lee, et al. Science 321 (2008) 385.
[6] T.J. Booth, et al. Nano Lett. 8 (2008) 2442–2446.
[7] J.S. Bunch, et al. Nano Lett. 8 (2008) 2458–2462.
[8] R.R. Nair, et al. Science 320 (2008) 1308.
[9] A.A. Balandin, et al. Nano Lett. 8 (2008) 902–907.
[10] K.S. Novoselov, et al. Proc. Natl. Acad. Sci. U. S. A. 102 (2005) 10451.
[11] Q.H. Wang, et al. Nat. Nanotechnol. 7 (2012) 699–712.
[12] M. Chhowalla, et al. Nat. Chem. 5 (2013) 263–275.
[13] V. Nicolosi, et al. Science 340 (2013) 1226419.
[14] L. Li, et al. Nat. Nanotechnol. 9 (2014) 372–377.
[15] C.N.R. Rao, H.S.S. Ramakrishna Matte, U. Maitra, Angew. Chem. 52 (2013) 13162–13185.
[16] M.J. Kory, et al. Nat. Chem. 6 (2014) 779–784.
[17] M. Buscema, et al. Chem. Soc. Rev. 44 (2015) 3691.
[18] J. Zupan, D. Kolar, J. Phys. C: Solid State Phys. 5 (1972) 3097–3100.
[19] S. Bae, et al. Nat. Nano 5 (2010) 574–578.
[20] W. Gannett, et al. Appl. Phys. Lett. 98 (2011) 242105.
[21] V.E. Calado, et al. Appl. Phys. Lett. 104 (2014) 023103.
[22] W. Yang, et al. Nat. Mater. 12 (2013), 792–292.
[23] Z. Liu, et al. Nat. Nanotechnol. 8 (2013) 119–124.
[24] K.I. Bolotin, et al. Solid State Commun. 146 (2008) 351–355.
[25] A.S. Mayorov, et al. Nano Lett. 12 (2012) 4629–4634.
[26] C.R. Dean, et al. Nat. Nanotechnol. 5 (2010) 722–726.
[27] A.F. Young, et al. Nat. Phys. 8 (2012) 550–556.
[28] C.R. Dean, et al. Nat. Phys. 7 (2011) 693–696.
[29] A. Kou, et al. Science 345 (2014) 55–57.
[30] P.J. Zomer, et al. Phys. Rev. B 86 (2012) 161416.
[31] A.F. Young, et al. Nature 505 (2014) 528–532.
[32] A.F. Young, et al. Phys. Rev. B 85 (2012) 235458.
[33] S. Dröscher, et al. New J. Phys. 14 (2012) 103007.
[34] J.Y. Tan, et al. Appl. Phys. Lett. 104 (2014) 183504.
[35] A. Avsar, et al. Nat. Commun. 5 (2014) 4875.
[36] S. Larentis, et al. Nano Lett. 14 (2014) 2039–2045.
[37] F. Schedin, et al. Nat. Mater. 6 (2007) 652–655.
[38] A.S. Mayorov, et al. Nano Lett. 11 (2011) 2396–2399.
[39] M.H.D. Guimaraes, et al. Phys. Rev. Lett. 113 (2014) 086602.
[40] J. Ingla-Aynes, et al. Phys. Rev. B 92 (2015), 201410(R).
[41] S.J. Haigh, et al. Nat. Mater. 11 (2012) 764–767.
[42] Z. Li, et al. Nat. Mater. 12 (2013) 925–931.
[43] L. Wang, et al. Science 342 (2013) 614–617.
[44] P.J. Zomer, et al. Appl. Phys. Lett. 105 (2014) 013101.
[45] V.E. Calado, et al. Nat. Nanotechnol. 10 (2015) 761.
[46] A.M. Goossens, et al. Nano Lett. 12 (2012) 4656–4660.
[47] E. McCann, Phys. Rev. B 74 (2006) 161403.
[48] E.V. Castro, et al. Phys. Rev. Lett. 99 (2007) 216802.
[49] J.B. Oostinga, et al. Nat. Mater. 7 (2007) 151–157.
[50] L. Ju, et al. Nature 520 (2015) 650–655.
[51] A. Varlet, et al. Phys. Rev. Lett. 113 (2014) 116601.
[52] A. Varlet, et al. Phys. Rev. Lett. 113 (2014) 116602.
[53] P. Maher, et al. Science 345 (2014) 61–64.
[54] M. Sui, et al. Nat. Phys. 11 (2015) 1027.
[55] Y. Shimazaki, et al. Nat. Phys. 11 (2015) 1032.
[56] M.T. Allen, et al. Nat. Phys. (2015) (advance online publication).
[57] M.T. Allen, J. Martin, A. Yacoby, Nat. Commun. 3 (2012) 934.
[58] G.-H. Lee, et al. Appl. Phys. Lett. 99 (2011) 243114.
[59] L. Britnell, et al. Nano Lett. 12 (2012) 1707–1710.
[60] T. Yamaguchi, et al. Appl. Phys. Lett. 105 (2014) 223109.
[61] T. Yamaguchi, et al. Appl. Phys. Express 6 (2013) 073001.
[62] L. Britnell, et al. Science 335 (2012) 947–950.
[63] T. Georgiou, et al. Nat. Nanotechnol. 8 (2013) 100–103.
[64] F. Schwierz, Nat. Nanotechnol. 5 (2010) 487–496.
[65] R.V. Gorbachev, et al. Nat. Phys. 8 (2012) 896–901.
[66] M. Titov, et al. Phys. Rev. Lett. 111 (2013) 166601.
[67] L.A. Ponomarenko, et al. Nat. Phys. 7 (2011) 958–961.
[68] J.M.B. Lopes dos Santos, N.M.R. Peres, A.H. Castro Neto, Phys. Rev. Lett. 99 (2007) 256802.
[69] C.R. Dean, et al. Nature 497 (2013) 598–602.
[70] L.A. Ponomarenko, et al. Nature 497 (2013) 594–597.
[71] L. Wang, et al., Fractional fractal quantum Hall effect in graphene superlattices., 2015 arXiv:1505.07180.
[72] R.V. Gorbachev, et al. Science 346 (2014) 448–451.
[73] Mark B. Lundeberg, Joshua A. Folk, Science 346 (2014) 422–423.
[74] M.S. Choi, et al. Nat. Commun. 4 (1624) 2013.
[75] G.-H. Lee, et al. ACS Nano 7 (2013) 7931–7936.

[76] C.-H. Lee, et al. Nat. Nanotechnol. 9 (2014) 676–681.
[77] D. Bischoff, et al. Phys. Rev. B 91 (2015) 115441.
[78] D. Bischoff, et al. Appl. Phys. Lett. 101 (2012) 203103.
[79] D. Bischoff, et al. Phys. Rev. B 90 (2014) 115405.
[80] Z. Chen, et al. Physica E 40 (2007) 228–232.
[81] M.Y. Han, et al. Phys. Rev. Lett. 98 (2007) 206805.
[82] T. Ihn, et al. Mater. Today 13 (2010) 44–50.
[83] D. Bischoff, et al. Appl. Phys. Rev. 2 (2015) 031301.
[84] S. Engels, et al. Appl. Phys. Lett. 103 (2013) 073113.
[85] D. Bischoff, et al. Nano Lett. 15 (2015) 6003.
[86] Y.Y. Wei, et al. Phys. Rev. Lett. 81 (1998) 1674–1677.
[87] H.F. Hess, et al. Solid State Commun. 107 (1998) 657–661.
[88] J. Martin, et al. Nat. Phys. 5 (2009) 669–674.
[89] S. Dröscher, et al. Phys. Scr. 146 (2012) 014009.
[90] G. Shi, et al. Nano Lett. 14 (2014) 1739–1744.
[91] R. Sanchez, Phys. Rev. Lett. 104 (2010) 076801.
[92] O. Zilberberg, A. Carmi, A. Romito, Phys. Rev. B 90 (2014) 205413.
[93] J. Güttinger, et al. Phys. Rev. B 83 (2011) 165445.
[94] D. Bischoff, et al. New J. Phys. 15 (2013) 083029.
[95] A.C. Ferrari, et al. Nanoscale 7 (2015) 4598.